New Series of Organogelators Derived from a Combinatorial Library of Primary Ammonium Monocarboxylate Salts

Amar Ballabh, Darshak R. Trivedi, and Parthasarathi Dastidar*

Analytical Science Discipline, Central Salt & Marine Chemicals Research Institute, G. B. Marg, Bhavnagar 364 002, Gujarat, India

Received March 1, 2006. Revised Manuscript Received June 9, 2006

A crystal engineering approach has been adopted to generate a combinatorial library of 40 primary ammonium monocarboxylate salts derived from 10 cinnamic acid derivatives and 4 *n*-alkyl primary amines, as potential organic gelators. It is observed that 4-Cl, 4-Me, and 4-Br cinnamate salts of $CH_3(CH_2)_n-NH_2$ ($n = 15$) are gelators. A systematic study of 4-Br cinnamate salts of *n*-alkylamine with varying chain lengths indicates that the alkyl chain length has a profound effect on gelation. A structure−property correlation study has been attempted on the basis of single-crystal and powder X-ray diffraction data of the salts.

Introduction

Low molecular mass organic gelators (LMOGs) are small organic molecules ($M_w < 1000$) capable of hardening various organic and aqueous fluids. LMOGs capable of gelling organic liquids, aqueous solvents (including pure water), and both organic and aqueous solvents are organogelators,[1] hydrogelators,[2] and ambidextrous gelling agents,[3] respectively. Supramolecular self-assembly leads to the formation of aggregates of gelator molecules into various morphologies such as fibers, strands, tapes, and so forth. Such aggregates are shown to cross-link among themselves through "junction zones"[4] to form a three-dimensional intertwined network of fibers within which the solvent molecules are immobilized resulting in gels or viscous liquids. Because various supramolecular events are responsible for the gelation process, such physical gels derived from LMOGs are often thermoreversible and at times display a thixotropy property. As a result of various potential applications, for example, as structure-directing agents (template) for making inorganic nanomaterials,[5] in making microcelluar materials,[6] in the CO_2 based coating process,[6] in making dye sensitized solar cells,[7] and in biomedical applications,[8] research on LMOGs has been an active research field in the recent years in materials science and supramolecular chemistry.

However, designing a gelator molecule is still a major challenge because the exact mechanism of gel formation is poorly understood. Moreover, the crystal structure of the gel fibers in the native gel state, which is understandably crucial for designing a LMOG, is virtually impossible to determine; only an indirect method using single-crystal X-ray data of the gelator in its neat crystalline form and X-ray powder diffraction (XRPD) data of gel fibers in the gel state may be applied.[9] However, recording good quality XRPD data of the gel fibers in its native form generally suffers from the scattering contribution of the solvent molecules and less crystalline nature of the gel fibers, and, therefore in most of the cases, attempts to record XRPD of gel fibers turn out to be a major disappointment.

After a serendipitous entry[10] to the field, we have shown[11] that the one-dimensional (1D) hydrogen bonded network observed in the neat crystalline state appears to be one of the prerequisites for gel formation, and, therefore, correlating the single-crystal structure of a molecule in its thermodynamically more stable crystalline state with its gelling/nongelling behavior seems to be more practical in designing new gelator molecules. It is quite logical to think that the driving forces for the growth of gel fibril in the fibril axis direction and perpendicular to it must be different because the growth in the former direction has to be faster than that in the latter direction to have 1D fiber morphology generally observed in scanning electron microscopy (SEM) micrographs of xerogels. The 1D hydrogen bonded network, thus, might play a significant role for the elongated growth of the

* To whom correspondence should be addressed. Fax: +91-278-2567562. E-mail: parthod123@rediffmail.com; dastidar@csmcri.org.

(1) For excellent reviews on LMOGs, see (a) Terech, P.; Weiss, R. G. *Chem. Rev.* **1997**, *97*, 3133. (b) Grownwald, O.; Shinkai, S. *Curr. Opin. Colloid Interface Sci.* **2002**, *7*, 148. (c) van Esch, J. H.; Ferringa, B. L. *Angew. Chem., Int. Ed.* **2000**, *39*, 2263. (d) Sangeetha, N. M.; Maitra, U. *Chem. Soc. Rev.* **2005**, *34*, 821.
(2) Estroff, L. A.; Hamilton, A. D. *Chem. Rev.* **2004**, *104*, 1201.
(3) Oda, R.; HUc, I.; Candau, S. J. *Angew. Chem., Int. Ed.* **1998**, *37*, 2689.
(4) (a) Terech, P.; Ostuni, E.; Weiss, R. G. *J. Phys. Chem.* **1996**, *100*, 3759. (b) Terech, P.; Furman, I.; Weiss, R. G. *J. Phys. Chem.* **1996**, *99*, 9958 and references therein.
(5) (a) Suzuki, M.; Nakajima, Y.; Sato, T.; Shirai, H.; Hanabusa, K. *Chem. Commun.* **2006**, 377. (b) Jung, J. H.; Shimizu, T.; Shinkai, S. *J. Mater. Chem.* **2005**, *15*, 3979.
(6) Shi, C.; Huang, Z.; Kilic, S.; Xu, J.; Enick, R. M.; Beckmann, E. J.; Carr, A. J.; Melendez, R. E.; Hamilton, A. D. *Science* **1999**, *286*, 1540.
(7) Kubo, W.; Kitamura, T.; Hanabusa, K.; Wada, Y.; Yanagida, S. *Chem. Commun.* **2002**, 374.
(8) (a) Wilder, E. A.; Wilson, K. S.; Quinn, J. B.; Skrtic, D.; Antonucci, J. M. *Chem. Mater.* **2005**, *17*, 2946. (b) Kiyonaka, S.; Sada, K.; Yoshimura, I.; Shinkai, S.; Kato, N.; Hamachi, I. *Nat. Mater.* **2004**, *3*, 58. (c) Kurisawa, M.; Chung, J. E.; Yang, Y. Y.; Gao, S. J.; Uyama, H. *Chem. Commun.* **2005**, 4312. (d) Lee, K. Y.; Mooney, D. J. *Chem. Rev.* **2001**, *101*, 1869. (e) Xing, B.; Yu, C.-W.; Chow, K.-H.; Ho, P.-L; Fu, D.; Xu, B. *J. Am. Chem. Soc.* **2002**, *124*, 14846. (f) Langer, R. *Acc. Chem. Res.* **2000**, *33*, 94.
(9) Ostuni, E.; Kamaras, P.; Weiss, R. G. *Angew. Chem., Int. Ed. Engl.* **1996**, *35*, 1324.
(10) Ballabh, A.; Trivedi, D. R.; Dastidar, P. *Chem. Mater.* **2003**, *15*, 2136.
(11) (a) Trivedi, D. R.; Ballabh, A.; Dastidar, P. *Chem. Mater.* **2003**, *15*, 3971. (b) Trivedi, D. R.; Ballabh, A.; Dastidar, P.; Ganguly, B. *Chem.—Eur. J.* **2004**, *10*, 5311.

10.1021/cm0605015 CCC: $33.50
Published on Web 07/18/2006

Scheme 1

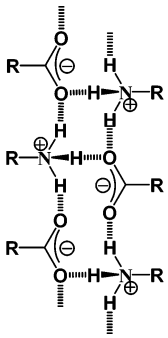

fibril in one direction while interactions with the solvent may prevent or reduce the growth perpendicular to the fibril axis.

Therefore, we have been actively engaged in exploiting supramolecular synthons[12] in synthesizing 1D hydrogen bonded networked organic solids as potential LMOGs.[13] In these studies, we chose to work with organic salts because salt preparation does not involve any time-consuming nontrivial organic synthesis; in a relatively short period of time, many salts can be prepared by following a combinatorial library approach[14] and scanned for gelation. Moreover, supramolecular assemblies in organic salts are based on strong directional hydrogen bonding and stronger less directional electrostatic interactions. Supramolecular synthons in organic salts are expected to be strong and robust. Thus, salt based LMOGs are increasingly becoming popular.[15] Primary alkylammonium monocarboxylate salts mostly display a ladder type 1D columnar hydrogen bonded network.[16] Our recent efforts to exploit such supramolecular synthon (Scheme 1) lead to the formation of a new class of organogelators capable of gelling various organic fluids including petrol instantaneously at room temperature[17] and nanotubular organogelators.[18]

Being encouraged with these results, we have decided to exploit the synthon further and have launched a systematic study to generate a new class of LMOGs based on organic salts. For this purpose, we have followed a combinatorial library approach. The combinatorial library was made by reacting 10 cinnamic acid derivatives and 4 alkylamines

Scheme 2

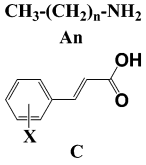

C1, X = 4-Cl; C2, X = 3-Cl; C3, X = 2-Cl
C4, X = 4-Me; C5, X = 3-Me; C6, X = 2-Me
C7, X = 4-Br; C8, X = 3-Br; C9, X = 2-Br
C10, X = H

Table 1. Combinatorial Library of Primary Ammonium Cinnamate Salts[a]

	A3	A4	A5	A15
C1	C1A3	C1A4	C1A5	**C1A15**
C2	C2A3	C2A4	C2A5	C2A15
C3	C3A3	C3A4	C3A5	C3A15
C4	C4A3	C4A4	C4A5	**C4A15**
C5	C5A3	C5A4	C5A5	C5A15
C6	C6A3	C6A4	C6A5	C6A15
C7	C7A3	C7A4	C7A5	**C7A15**
C8	C8A3	C8A4	C8A5	C8A15
C9	C9A3	C9A4	C9A5	C9A15
C10	C10A3	C10A4	C10A5	C10A15

[a] Salts shown in bold are gelators.

(Scheme 2, Table 1). In this article, we report a new class of organogelators that emerged from the combinatorial library. We also report a systematic structure−property correlation study based on the single-crystal X-ray diffraction and XRPD data of gelator and nongelator salts.

Results and Discussions

Gel Formation and Characterization. The salts in the combinatorial library (Table 1) were quickly scanned for gelation with a few prototype solvents normally used for gelation studies.[14a] In a typical experiment, a salt is dissolved in a suitable solvent with the aid of a few drops of good solvent (MeOH) and heating. The solution is then allowed to cool to room temperature under ambient conditions. The container (usually a test tube) is then inverted to examine the material's deformity. If no deformation is observed, it is considered a gel. It was found by scanning the combinatorial library that three salts, namely, **C1A15**, **C4A15**, and **C7A15**, showed gelation property. Table 2 enlists the gelation data of these salts. It is clear from this table that the gelators are capable of gelling both polar and nonpolar solvents including commercial fuels such as kerosene, petrol, and diesel with remarkable efficiency (minimum gelator concentration, MGC $= \sim 0.47-2.68$ wt %) and stability ($T_{gel} = 48-72$ °C).

SEM micrographs (Figure 1) of the xerogels of **C1A15**, **C4A15**, and **C7A15** in various solvents display a typical intertwined network of fibers within which the solvent molecules are understandably immobilized to form gel.

Interestingly, salts **C1A15**, **C4A15**, and **C7A15** display the ability to gel commercial fuels (petrol, kerosene, and diesel) selectively from the corresponding oil/water mixtures. While **C4A15** and **C7A15** display selective gelation of petrol, diesel, and kerosene, **C1A15** is able to gel petrol and diesel selectively from the corresponding oil/water mixtures. In a typical experiment, the gelator salt is dissolved in a mixture of oil/water (1:1, v/v) with the help of few drops of MeOH

(12) Desiraju, G. R. *Angew. Chem.* **1995**, *107*, 2541; *Angew. Chem., Int. Ed. Engl.* **1995**, *34*, 2311.
(13) (a) Trivedi, D. R.; Ballabh, A.; Dastidar, P. *J. Mater. Chem.* **2005**, *15*, 2606. (b) Ballabh, A.; Trivedi, D. R.; Dastidar, P. *Cryst. Growth Des.* **2005**, *5*, 1545. (c) Trivedi, D. R.; Ballabh, A.; Dastidar, P. *Crystal Growth Des.* **2006**, *6*, 673. (d) Trivedi, D. R.; Dastidar, P. *Chem. Mater.* **2006**, in press.
(14) (a) Dastidar, P.; Okabe, S.; Nakano, K.; Iida, K.; Miyata, M.; Tohnai, N.; Shibayama, M. *Chem. Mater.* **2005**, *17*, 741. (b) Nakano, K.; Hishikawa, Y.; Sada, K.; Miyata M.; Hanabusa, K. *Chem. Lett.* **2000**, 1170.
(15) (a) Ayabe, M.; Kishida, T.; Fujita, N.; Sada, K.; Shinkai, S. *Org. Biomol. Chem.* **2003**, *1*, 2744. (b) Abdallah, D. J.; Weiss, R. G. *Chem. Mater.* **2000**, *12*, 406, (c) George, M.; Weiss, R. G. *J. Am. Chem. Soc.* **2001**, *11*, 10393. (d) George, M.; Weiss, R. G. *Langmuir* **2003**, *19*, 1017.
(16) (a) Chenug, E.; Rademacher, K.; Scheffer, J. R.; Trotter, J. *Tetrahedron Lett.* **1999**, *40*, 8733. (b) Kinbara, K.; Kai, A.; Maekawa, Y.; Hashimoto, Y.; Naruse, S.; Hasegawa, M.; Saigo, K. *J. Chem. Soc., Perkin Trans.* 2 **1996**, 247. (c) Kinbara, K.; Hashimoto, Y.; Sukegawa, M.; Nohira, H.; Saigo, K. *J. Am. Chem. Soc.* **1996**, *118*, 3441. (d) Kinbara, K.; Tagawa, Y.; Saigo, K. *Tetrahedron: Asymmetry* **2001**, *12*, 2927.
(17) Trivedi, D. R.; Dastidar, P. *Chem. Mater.* **2006**, in press.
(18) Ballabh, A.; Trivedi, D. R.; Dastidar, P. *Org. Lett.* **2006**, in press.

Table 2. Gelation Data of Salts C1A15, C4A15, and C7A15[a]

	C1A15		C4A15		C7A15	
solvent	MGC (wt %)	T_{gel} (°C)	MGC (wt %)	T_{gel} (°C)	MGC (wt %)	T_{gel} (°C)
CCl_4	2.68	68	not done		1.31	50
cyclohexane	1.14	61	0.48	63	0.97	60
n-hexane	FC		0.87	70	2.28	62
n-heptane	1.07	72	1.48	62	1.17	64
n-octane	P		0.69	50	1.46	*b*
isooctane	2.28	59	0.47	68	1.92	72
n-decane	P		1.05	57	1.05	*b*
kerosene	P		1.00	55	1.26	54
petrol	0.68	55	0.81	53	1.41	56
diesel	1.12	68	1.57	58	1.20	66
parrafin	0.91	65	0.47	56	VL	
benzene	1.17	48	P		1.29	52
toluene	1.64	62	1.24	51	1.08	54
chlorobenzene	1.47	52	FC		1.14	50
bromobenzene	1.12	50	FC		1.12	60
o-xylene	P		1.08	56	1.12	54
m-xylene	P		1.18	52	1.03	54
p-xylene	1.15	64			1.05	56
mesitelene	1.22	63	1.33	48	1.07	58
methyl salisilate	FC		0.53	52	1.02	*b*
1,2-dichlorobenzene	1.09	58			1.04	56
nitrobenzene	S		0.51	66	1.16	62
coconut oil	not done				1.22	60
1,4-dioxane	S		1.21	51	1.08	48

[a] FC, fibrous crystals; P, precipitate; S, solution; and VL, viscous liquid. [b] T_{gel} not measured because of instability.

and heating. The mixture is then kept for equilibration at room temperature. After a few hours, the oil layers are found be gelled completely, leaving the water phases unaffected (Figure 2). Selective gelation of oil from an oil/water mixture is considered important in containing the oil spill problem.[11,19]

It is also clear from Table 2 that both the 4-substituents of the carboxylate moiety and the long alkyl chain of the ammonium moiety appear to have a profound effect on gelation. To check the threshold of the alkyl chain length of the ammonium moiety on gelation, we chose to work systematically with 4-bromocinnamic acid **C7** and alkylamines with varying chain lengths. For this purpose, we prepared a series of salts **C7A*n*** ($n = 3-15$) and checked their gelation properties. Salts **C7A*n*** ($n = 3-6$) are nongelators, and salts **C7A*n*** ($n = 7-15$) are gelators of which salts **C7A*n*** ($n = 11-15$) are better gelators (Table 3). These results indicate that the long alkyl chain of the amine moiety plays a significant role in the gelling properties of the corresponding salts.

Structure−Property Correlation. In an attempt to correlate the single-crystal structure of salt with its gelling/nongelling property, efforts were made to crystallize as many salts as possible. Thus, 11 nongelator and 4 gelator salts could be crystallized for single-crystal X-ray diffraction studies. Crystallographic parameters are listed in Table 4.

The nongelator salts belong in the centrosymmetric triclinic space group $P\bar{1}$, except for salt **C10A3**, which crystallizes in the noncentrosymmetric orthorhombic space group $P2_12_12_1$. On the other hand, gelator salts mostly display the centrosymmetric monoclinic space group $P2_1/c$, except for **C7A10**, which shows centrosymmetric orthorhombic space group *Pbca*. The asymmetric unit of all the salts contains one ion pair. It is intriguing to note that all the salts, irrespective of their properties (gelling/nongelling), display a 1D hydrogen bonded network as envisaged for primary ammonium monocarboxylate salts (Scheme 1). Within the networks, the ion pairs are strongly held together by N−H···O hydrogen bonding [range N···O = 2.724(2)−3.054(11) Å; ∠N−H···O = 143.2(2)−178.0(3)°; Table S1, Supporting Information].

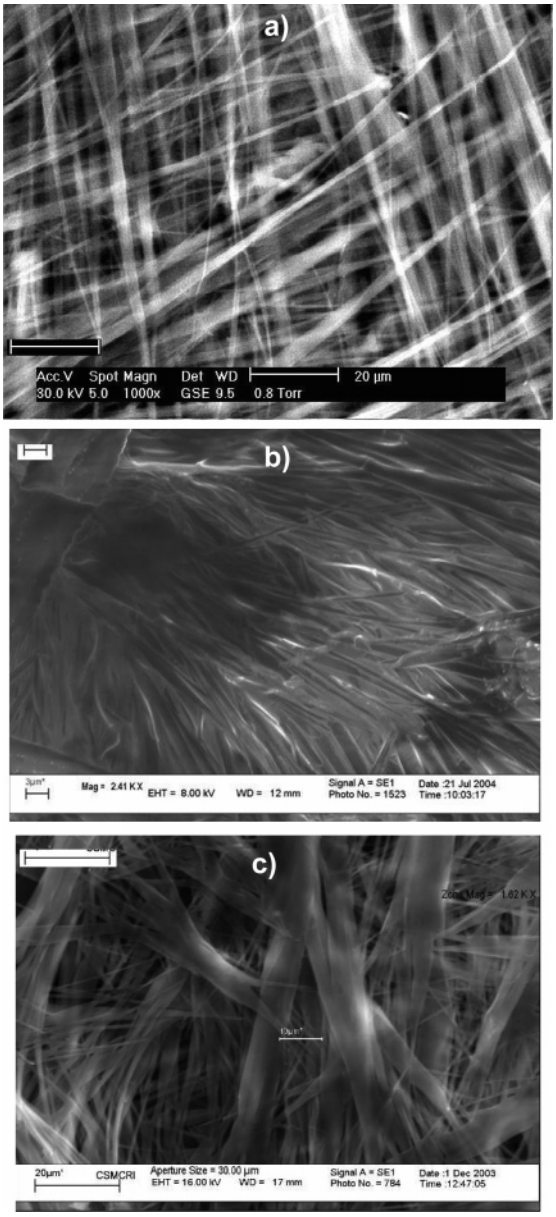

Figure 1. SEM micrographs of xerogels: (a) 2.5 wt % **C1A15** in *p*-xylene (bar = 10 μm); (b) 2.5 wt % **C4A15** in diesel (bar = 3 μm); and (c) 1.0 wt % **C7A15** in *n*-heptane (bar = 20 μm).

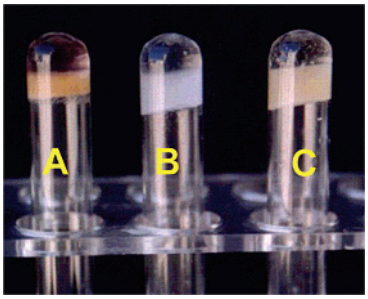

Figure 2. Selective gelation of oil from oil/water mixtures by **C7A15**: (a) petrol; (b) kerosene, and (c) diesel. It can be seen that the top water layers remain unaffected.

(19) (a) Bhattacharya, S.; Krishnan-Ghosh, Y. *Chem. Commun.* **2001**, 185. (b) Freemantle, M. *Chem. Eng. News* **2001**, *79*, 12.

Table 3. Gelation Data of Salts of 4-Bromocinnamic Acid with *n*-Alkylamine Having Varying Chain Lengths[a,b]

	C7A14		C7A13		C7A12		C7A11		C7A10		C7A9		C7A8		C7A7	
solvent	MGC (wt %)	T_{gel} (°C)	MGC (wt %)	T_{gel} (°C)	MGC (wt %)	T_{gel} (°C)	MGC (wt %)	T_{gel} (°C)	MGC (wt %) w/v	T_{gel} (°C)	MGC (wt %) w/v	T_{gel} (°C)	MGC (wt %) w/v	T_{gel} (°C)	MGC (wt %) w/v	T_{gel} (°C)
CCl_4	1.49	48	1.50	48	1.50	*c*	1.47	50	P		1.48	42	P		1.51	48
cyclohexane	1.44	58	1.48	62	1.59	62	1.50	60	1.50	58	1.39	58	1.76	44	0.85	68
n-hexane	3.66	68	2.37	70	WG		WG		3.81	*c*	WG		FC		FC	
n-heptane	1.17	60	1.05	68	1.21	*c*	WG		2.85	*c*	2.75	*c*	FC		FC	
n-octane	1.11	60	1.11	46	WG		WG		WG		FC		FC		FC	
isooctane	1.279	60	1.29	*c*	WG		1.29	*c*	FC		P		FC		FC	
n-decane	WG		WG		FC		1.25	50	WG		VL		FC		FC	
kerosene	WG		WG		P		P		FC		P		P		P	
petrol	1.41	50	1.42	58	WG		1.45		2.68	*c*	FC		P		FC	
diesel	WG		1.18	65	P		1.20		FC		P		FC		P	
paraffin liq.	VL		VL		VL		VL		P		P		P		P	
benzene	1.27	44	1.34	*c*	1.30	42	1.35	44	P		P		P		1.49	46
toluene	P		1.10	*c*	WG		1.11	44	P		P		P		1.10	50
chlorobenzene	1.01	44	WG		WG		WG		FC		P		P		WG	
bromobenzene	WG		WG		WG		WG		WG		WG		P		FC	
o-xylene	WG		WG		WG		FC		WG		WG		FC		FC	
m-xylene	VL		WG		WG		WG		WG		WG		FC		P	
p-xylene	FC		WG		P		2.45	42	WG		FC		FC		P	
mesitylene	1.16	44	WG		1.99	50	1.18	48	P		VL		VL		1.516	*c*
methyl salicylate	VL		S		S		S		FC		P		FC		P	
1,2-dichlorobenzene	VL		S		VL		P		FC		VL		FC		VL	
DMSO	VL		S		S		S		S		S		S		S	
nitrobenzene	VL		VL		P		P		FC		FC		FC		FC	
coconut oil[d]	P		P		P		P		P		P		P		P	
1,4-dioxane	P		P		P		P		P		P		P		P	

[a] WG, weak gel; VL, viscous liquid; P, precipitate; S, solution; and FC, fibrous crystals. [b] MGC = amount of gelator required for gelling 1 mL of solvent (w/v %); T_{gel} = temperature at which the gel changes into a sol. [c] T_{gel} not measured because of instability. [d] MGC in wt of gelator/wt of solvent (w/w %).

Table 4. Crystallographic Data

crystal data	C1A3	C1A4	C1A5	C4A5	C7A3	C7A4	C7A5
empirical formula	$C_{13}H_{18}ClNO_2$	$C_{14}H_{20}ClNO_2$	$C_{15}H_{22}ClNO_2$	$C_{16}H_{25}NO_2$	$C_{26}H_{36}Br_2N_2O_4$	$C_{28}H_{40}Br_2N_2O_4$	$C_{30}H_{44}Br_2N_2O_4$
fw	255.73	269.76	283.79	263.37	600.39	628.44	656.49
crystal size (mm)	0.38 × 0.27 × 0.09	0.43 × 0.28 × 0.08	0.24 × 0.16 × 0.15	0.49 × 0.28 × 0.08	1.19 × 0.27 × 0.11	0.32 × 0.30 × 0.06	0.92 × 0.28 × 0.16
crystal system	triclinic	triclinic	triclinic	triclinic	triclinic	triclinic	triclinic
space group	$P\bar{1}$	$P\bar{1}$	$P\bar{1}$	$P\bar{1}$	$P\bar{1}$	$P\bar{1}$	$P\bar{1}$
a (Å)	5.5431(11)	5.5410(13)	5.5021(8)	5.5328(7)	5.5628(4)	5.5611(10)	5.5215(5)
b (Å)	7.4791(14)	7.4502(18)	7.4745(11)	7.5138(9)	7.5055(5)	7.4809(13)	7.5087(6)
c (Å)	16.190(3)	17.662(4)	19.108(3)	19.059(2)	16.4604(11)	17.889(3)	19.0830(16)
α (deg)	82.779(3)	90.182(5)	92.671(3)	92.937(2)	82.4490(10)	88.908(3)	93.1300(10)
β (deg)	88.900(4)	92.714(4)	90.828(3)	90.228(2)	88.7850(10)	87.831(3)	90.752(2)
γ (deg)	71.490(3)	108.560(4)	107.964(2)	108.446(2)	71.4810(10)	71.593(3)	108.1310(10)
volume (Å^3)	631.3(2)	690.3(3)	746.36(19)	750.45(16)	645.86(8)	705.6(2)	750.38(11)
Z	2	2	2	2	1	1	1
D_{calcd}	1.345	1.298	1.263	1.166	1.544	1.479	1.453
F(000)	272	288	304	288	308	324	340
Mo Kα (mm^{-1})	0.293	0.271	0.254	0.076	3.173	2.908	2.737
temperature (K)	293(2)	293(2)	293(2)	293(2)	100(2)	100(2)	293(2)
observed reflections [$I > 2\sigma(I)$]	1498	1535	1285	1602	2782	2831	3189
parameters refined	167	176	185	186	226	243	260
goodness of fit	1.121	1.086	1.184	1.023	1.028	1.069	1.069
final R_1 on observed data	0.0529	0.0418	0.0740	0.0414	0.0236	0.0290	0.0259
final wR_2 on observed data	0.1522	0.1115	0.2230	0.1011	0.0655	0.0720	0.0747

crystal data	C7A6	C8A3	C8A5	C10A3	C7A9	C7A10	C7A11	C7A13
empirical formula	$C_{32}H_{48}Br_2N_2O_4$	$C_{26}H_{36}Br_2N_2O_4$	$C_{30}H_{44}Br_2N_2O_4$	$C_{13}H_{15}NO_2$	$C_{19}H_{30}BrNO_2$	$C_{20}H_{32}BrNO_2$	$C_{21}H_{34}BrNO_2$	$C_{23}H_{38}BrNO_2$
fw	684.54	600.39	656.49	217.26	384.35	398.38	412.40	440.45
crystal size (mm)	1.03 × 0.78 × 0.07	1.28 × 0.44 × 0.2	0.57 × 0.23 × 0.2	0.86 × 0.30 × 0.2	1.05 × 0.67 × 0.12	0.97 × 0.56 × 0.12	0.97 × 0.47 × 0.23	1.22 × 0.82 × 0.02
crystal system	triclinic	triclinic	triclinic	orthorhombic	monoclinic	orthorhombic	monoclinic	monoclinic
space group	$P\bar{1}$	$P\bar{1}$	$P\bar{1}$	$P2_12_12_1$	$P2_1/c$	*Pbca*	$P2_1/c$	$P2_1/c$
a (Å)	5.5753(11)	5.5484(5)	5.5108(8)	6.2089(7)	24.134(7)	14.342(2)	26.525(4)	28.972(4)
b (Å)	7.7318(15)	7.4632(7)	7.5698(11)	8.9509(11)	14.298(4)	5.7760(8)	14.2644(19)	14.2687(17)
c (Å)	20.485(4)	16.9022(16)	19.051(3)	23.295(3)	5.8109(17)	51.085(7)	5.7997(8)	5.7800(7)
α (deg)	87.193(3)	90.896(2)	82.296(3)	90.00	90.00	90.00	90.00	90.00
β (deg)	88.939(3)	99.105(2)	82.827(2)	90.00	91.786(5)	90.00	93.063(2)	95.027(2)
γ (deg)	72.223(3)	107.802(2)	72.395(2)	90.00	90.00	90.00	90.00	90.00
volume (Å^3)	839.9(3)	656.46(11)	747.67(19)	1294.6(3)	2004.1(10)	4231.9(10)	2191.2(5)	2380.2(5)
Z	1	1	1	4	4	8	4	4
D_{calcd}	1.353	1.519	1.458	1.115	1.274	1.251	1.250	1.229
F(000)	356	308	340	464	808	1680	872	936
Mo Kα (mm^{-1})	2.449	3.121	2.747	0.075	2.060	1.954	1.889	1.743
temperature (K)	293(2)	100 (2)	293(2)	293(2)	293(2)	293(2)	293(2)	293(2)
observed reflections [$I > 2\sigma(I)$]	2614	2773	3105	2862	3054	2064	3556	3393
parameters refined	194	156	260	166	210	213	228	246
goodness of fit	0.974	1.058	1.134	1.095	1.009	1.168	1.006	0.988
final R_1 on observed data	0.0448	0.0420	0.0304	0.0480	0.0438	0.0664	0.0422	0.0474
final wR_2 on observed data	0.1139	0.1136	0.0847	0.1393	0.1025	0.1693	0.1056	0.1015

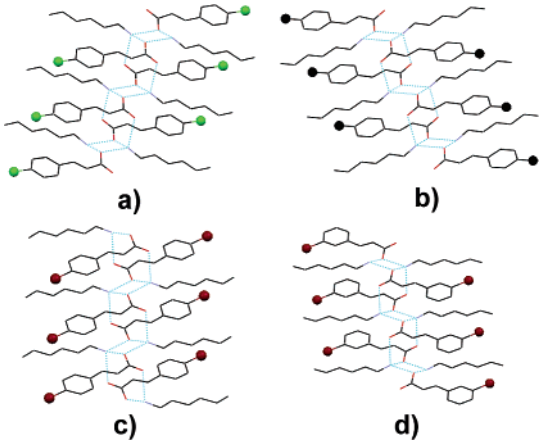

Figure 3. Illustration of crystal structures depicting a 1D hydrogen bonded network and the relative arrangement of the ionic moieties along the network: (a) **C1A5**, (b) **C4A5**, (c) **C7A5**, and (d) **C8A5**.

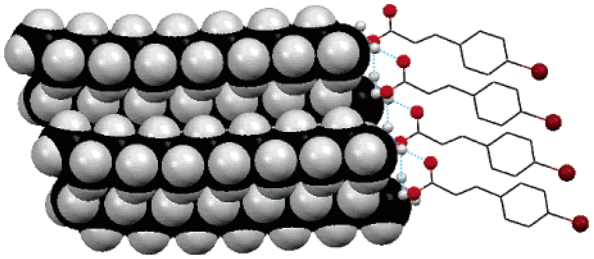

Figure 4. Illustration of the crystal structure depicting intranetwork alkyl−alkyl interactions in **C7A13**; salts **C7A9** and **C7A11** display identical netwoks.

Analyses of the structures reveal that, in the nongelator salts, both the cationic and anionic moieties are centrosymmetrically located on the 1D columnar hydrogen bonded network, meaning that alkyl chains of the cationic moieties are not able to interact with each other within the network. Various substituents on the cinnamate moiety do not appear to have any effect on the relative arrangement of the cation and anion along the hydrogen bonded network. Figure 3 depicts identical network structures in salts **C1A5**, **C4A5**, **C7A5**, and **C8A5**, emphasizing these results.

On the other hand, in the gelator salts **C7A9**, **C7A11**, and **C7A13**, the cationic and anionic moieties are positioned on the same side of the 1D columnar hydrogen bonded network respectively meaning that the relatively long alkyl chains of the cationic moieties in these salts are favorably situated for alkyl−alkyl interactions within the network. Figure 4 displays alkyl−alkyl interactions in the hydrogen bonded network in **C7A13** emphasizing these results.

It may be noted that alkyl−alkyl interactions driven by relatively longer alkyl chains in gelator salts compared to that present in nongelator salts might be one of the driving forces for such an arrangement of the ionic moieties on the 1D hydrogen bonded network in these gelator salts. However, gelator salt **C7A10** displays an arrangement of ionic moieties on the hydrogen bonded network identical to that seen in nongelator salts as shown in Figure 3.

It may be important to note that the crystal structures of gelator salts reported herein do not display any halogen···halogen contacts.[20] On the other hand, few nongelator salts, namely, **C1A4**, **C8A5**, and **C7A4**, show significant halogen···halogen contacts (Cl···Cl = 3.402 Å in **C1A4**; Br···Br = 3.480 Å in **C7A4**; Br···Br = 3.574 Å in **C8A5**).

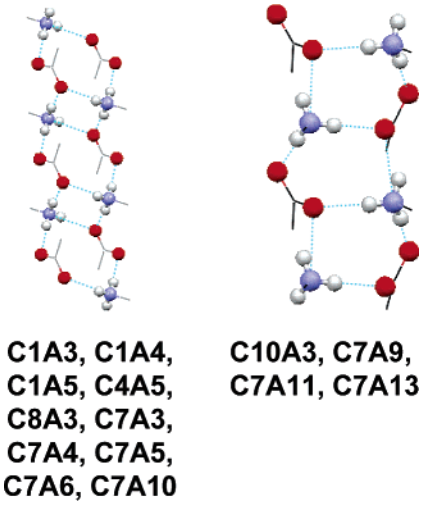

Figure 5. Supramolecular connectivities observed within the 1D hydrogen bonded network in the salts reported herein.

Careful analyses reveal that there are two types of supramolecular connectivities within the 1D columnar hydrogen bonded network (Figure 5).

All the nongelator salts except **C10A3** display a supramolecular connectivity within the 1D hydrogen bonded network, wherein alternating 8- and 12-membered rings of hydrogen bonded ion pairs are observed. **C10A3**, on the other hand, displays a supramolecular connectivity within the 1D network wherein identical hydrogen bonded 10-membered rings each comprising two anions and two cations are observed. The same supramolecular connectivity is also displayed by three gelator salts, namely, **C7A9**, **C7A11**, and **C7A13**. Gelator salt **C7A10**, on the other hand, displays the identical supramolecular connectivity displayed by most of the nongelator salts.

Thus, it is clear from single-crystal diffraction studies that all the salts irrespective of their gelling/nongelling behavior display a 1D hydrogen bonded network. It is also interesting to note that most of the nongelator and gelator salts display different supramolecular connectivities within the network. The most obvious question that needs to be addressed is why all the salts do not show gelation property despite having a 1D hydrogen bonded network. It may be emphasized here that the 1D hydrogen bonded network is one of the prerequisites for a molecule to be a gelling agent. It is logical to think that formation of a 1D fiberlike growth of gel fibers as frequently observed in SEM micrographs needs a driving force which could be a 1D hydrogen bonded network formation. While the 1D hydrogen bonded network might stimulate the growth in the fiber axis direction, interactions with solvent molecules perpendicular to it might slow the growth in this direction resulting in 1D fiber morphology with a very high aspect ratio. Moreover, the intertwined network of the gelator fiber should be able to immobilize the flow of solvent via surface tension or capillary force action. Therefore, surface compatibility of the solvent used in this study with the gel fiber should be achieved.

(20) Moorthy, J. N.; Natarajan, R.; Mal, P.; Venugopalan, P. *J. Am. Chem. Soc.* **2002**, *124*, 6530 and references cited therein.

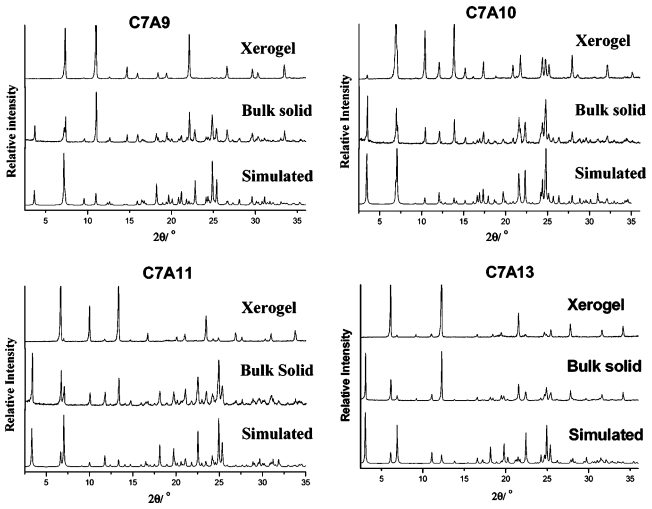

Figure 6. XRPD patterns of gelator salts under various conditions; xerogels prepared are from 1.0 wt % **C7A9** in cyclohexane, 1.0 wt % **C7A10** in cyclohexane, 1.0 wt % **C7A11** in carbon tetrachloride, and 1.0 wt % **C7A13** in carbon tetrachloride.

Understandably this could be one of the plausible reasons for nongelling behavior of the salts having a 1D hydrogen bonding network.

To see whether single-crystal structures of the gelator salts really represent that of the gel fibers or not, XRPD patterns generated by simulating single-crystal data, those of the bulk solid and xerogels, are compared for these gelator salts. It is clear from Figure 6 that simulated and bulk solid XRPD patterns are nearly identical in all the cases, meaning that the molecular packing obtained from single-crystal data indeed represents that in the bulk solid. However, the low angle peaks observed in both simulated and bulk solid are missing in xerogel XRPDs in all the cases, and also the wide angle region peaks in xerogels do not correspond well with that in simulated and bulk solid XRPDs indicating a different crystal structure of the gel fibers in the xerogel state. Solvent evaporation during xerogel formation may induce new nucleation events by crystallizing out some dissolved gelator molecules in the solvent, and, therefore, the new crystal phase in the xerogel different from that obtained in neat single-crystal form is not surprising. However, it should be emphasized here that the hydrogen bonded network in the fibers of xerogels may still be 1D as envisaged from the supramolecular synthon; only the packing of such a network may be different in the new crystal phase.

Conclusions

Thus, we have successfully demonstrated the aptitude of supramolecular synthon concepts in designing new LMOGs. A combinatorial library approach is followed to find a new series of gelling agents in a rational manner in a relatively short period of time. Some of the gelators, namely, **C1A15**, **C4A15**, and **C7A15**, display interesting selective gelation of commercial fuels (petrol, kerosene, and diesel) from the corresponding oil/water mixtures. A systematic structure−property correlation study on 4-bromocinnamate salt indicates that the chain length of the ammonium moiety has a profound effect on the gelation ability. Single-crystal structures the salts display a 1D columnar hydrogen bonded network irrespective of their properties (gelling/nongelling), indicating that the 1D hydrogen bonded network is only one of the prerequisites for gelation and not a necessary and sufficient condition. It may be stated in this context that single-crystal structures of a few gelators are also reported to be a 1D hydrogen bonded network.[21] XRPD studies indicate that the crystal phases of the fibers in the xerogels of 4-bromocinnamate gelators are different from that obtained in their corresponding neat single-crystal forms. The facile syntheses of the series of organogelators exploiting the concept of noncovalent synthesis (supramolecular synthesis) presented here should encourage chemists working in the area of design and synthesis of organic functional materials.

Experimental Section

Materials and Physical Measurements. All chemicals (Aldrich) and the solvents used for gelation (A.R. grade, S. D. Fine Chemicals, India) are used without further purification. All the oils were procured from the local market. Microanalyses are performed on a Perkin-Elmer elemental analyzer 2400, Series II. Fourier transform infrared (FT-IR) and ^{1}H NMR spectra are recorded using Perkin-Elmer Spectrum GX and 200 MHz Bruker Avance DPX200 spectrometers, respectively. XRPD patterns are recorded on a XPERT Philips (Cu Kα radiation) diffractometer. SEM is performed on a LEO 1430VP.

Preparation of Salts. All the salts are prepared by mixing equimolecular amounts of the corresponding acid and amine in the appropriate solvent followed by evaporation at ambient conditions at room temperature. The resultant white solid is isolated as the salt in a near quantitative yield. FT-IR spectra (KBr) of the salts show the presence of an asymmetric stretching band of the COO^- group at $\sim$1635 cm^{-1}, and the absence of the carbonyl (C═O) stretching band of COOH at $\sim$1690 cm^{-1} indicates complete salt formation.

Single-Crystal X-ray Diffraction. Diffraction data are collected using Mo Kα (λ = 0.7107 Å) radiation on a SMART APEX diffractometer equipped with a charge-coupled device area detector. Data collection, data reduction, and structure solution/refinement are carried out using the software package of SMART APEX.

All structures are solved by direct methods and refined in a routine manner. In all cases, nonhydrogen atoms are treated anisotropically, and the hydrogen atoms attached to nitrogen are located on a difference Fourier map and refined. The other hydrogen atoms are geometrically fixed.

During the refinement of **C10A3**, two unaccounted electron density peaks ($\sim$1.50 e/Å^{-3}) near the butyl chain are observed in the difference Fourier map. These electron densities are assigned as disordered carbon atoms coming from two methylene groups of the butyl chain. The second variable FVAR facility SHELXTL suite supplied as the APEX package is used to refine the occupancy of these disordered carbons atoms.

Acknowledgment. Ministry of Environment and Forests, New Delhi, India, is thankfully acknowledged for financial support. D.R.T. thanks CSIR for a SRF fellowship.

Supporting Information Available: Hydrogen bonding parameters (PDF) and crystallographic information (CIF). This material is available free of charge via the Internet at http://pubs.acs.org.

CM0605015

(21) Shirakawa, M.; Kawano, S.-i.; Fujita, N.; Sada, K.; Shinkai, S. *J. Org. Chem.* **2003**, *68*, 5037.